

AN UNTRAINED AND UNSUPERVISED METHOD FOR MRI BRAIN TUMOR SEGMENTATION

Tom Haeck^{a,b} Frederik Maes^{a,b} Paul Suetens^{a,b,c}

^a KU Leuven, Dept. of Electrical Engineering, ESAT-PSI, Leuven, Belgium

^b UZ Leuven, Medical Imaging Research Center, Leuven, Belgium

^c iMinds - Medical Information Technologies, Belgium

ABSTRACT

We present a fully-automated MRI brain tumor segmentation method that does not require any manually annotated training data. The method is independent of the scanner or acquisition protocol and is directly applicable to any individual patient image. An Expectation Maximization-approach is used to estimate intensity models for both normal and tumorous tissue. The segmentation is represented by a level-set that is iteratively updated to label voxels as normal or tumorous, based on which intensity model explains the voxels' intensity the best. The method is compared with the method by Menze et al. [1], which is considered to be a benchmark for unsupervised tumor segmentation. The performance of our method for segmenting the tumor volume is summarized by an average Dice score of 0.87 ± 0.06 on the training data set of the MICCAI BraTS Challenge 2012-2013.

Index Terms— brain tumor, segmentation, unsupervised, level-set, Expectation Maximization

1. INTRODUCTION

In current clinical practice, MR brain tumor images are assessed visually or assessed by using basic quantitative measures such as largest diameter to make a diagnosis or assess a treatment. This approach is time-consuming and has drawbacks regarding reproducibility and interrater-variability. Development of interactive or fully-automated MRI brain tumor segmentation methods is an ongoing field of research. By comparing manual segmentations from individual raters with the consensus segmentation of a group of raters, an upper limit for the performance of (semi-)automated methods is derived in Menze et al. [2]. It is shown that state-of-the-art segmentation methods still underperform significantly compared to this upper limit and more effort is needed to bring the methods into daily clinical practice.

We present an untrained and unsupervised MRI brain tumor segmentation method, i.e. no manually annotated training data is required and the tumor is segmented without any user interaction. The method is independent of the scanner

or acquisition protocol and is directly applicable to any individual patient image. Hence, the method is well suited for clinical or research settings for which only a limited amount of patient images needs to be segmented, no training data is available or there is insufficient manpower to annotate the training data that is available. Instead of relying on annotated training data, explicit prior knowledge of anatomy is incorporated into the algorithm in the form of a brain atlas [3]. The atlas is used for building a patient-specific intensity model for the normal tissue regions. Simultaneously, an intensity model is estimated for the tumorous region. A level-set is iteratively updated to label voxels as normal or tumorous, based on which intensity model explains the voxels' intensity the best. The problem is formulated as an L_1 -regularized optimization problem and is solved by a split Bregman iteration technique [4], which guides the search for tumorous voxels in a global way and independently of a manual initialization.

The performance of the method for segmenting the tumor volume is compared to the method by Menze et al. [1], which was awarded the Young Scientist Publication Impact Award 2015 by the MICCAI Society. Menze et al. present a fully Bayesian tumor segmentation framework, in which presence or absence of tumor in a voxel is represented by a hidden variable for which the posterior probability is estimated together with the image intensity model parameters. In Sec. 2, an overview of the method as well as a brief summary of the method by Menze et al. is provided. Both methods are compared by use of the training data of the MICCAI BraTS Challenge 2012-2013 in Sec. 3 and the results are discussed in Sec. 4. For notational simplicity, the method presented in this work will be called the split Bregman method, whereas the method by Menze et al. will be referred to as the Bayesian method from here onwards.

2. METHOD

Given is a multi-channel image $I : [0, 1]^d \rightarrow \mathbb{R}^C$ with C the number of channels. For both the Bayesian and the split Bregman method, the image intensities observed at voxel i are denoted by $\mathbf{y}_i = [y_1, \dots, y_C]^T$. The prior probability

that voxel i belongs to healthy tissue class k is given by a probabilistic brain atlas,

$$p(\Gamma_i = k) = \pi_{ik}, \quad k = 1, \dots, K, \quad (1)$$

,which is non-rigidly registered to the image I in a pre-processing step.

2.1. Bayesian method

For reasons of self-containment, this section provides a short summary on the Bayesian method. An explicit statistical model of an MR brain tumor image is built. By fitting this model to the tumor image at hand, a segmentation of the tumor is obtained.

Different channels show different patho-physiological processes and for this reason, tumor is not always as visible across channels. The tumor state $t_i^c \in \{0, 1\}$ indicates whether the tumor is visible in channel c . The overall unknown tumor state of a voxel i is thus given by the vector $\mathbf{t}_i = [t_i^1, \dots, t_i^C]^T$. The probability of having a tumor state \mathbf{t}_i is given by the Bernoulli distribution

$$p(\mathbf{t}_i | \alpha_i) = \prod_c \alpha_i^{t_i^c} (1 - \alpha_i)^{1 - t_i^c}, \quad (2)$$

with α_i a spatially varying tumor probability atlas that is shared across channels. The image intensity of a voxel i is assumed to be drawn from a probability distribution

$$p(\mathbf{y}_i | \mathbf{t}_i, k_i, \Theta) = \prod_c \left[\mathcal{N}(y_i^c; \Theta_k^c)^{1 - t_i^c} \mathcal{N}(y_i^c; \Theta_{K+1}^c)^{t_i^c} \right], \quad (3)$$

with $\mathcal{N}(\cdot; \Theta_k^c)$ a univariate Gaussian distribution with mean and variance summarized by Θ . Thus, the joint probability of the observed intensities in voxel i , its tumor state and the normal tissue class classification is given by

$$p(\mathbf{y}_i, \mathbf{t}_i, k_i | \Theta, \alpha_i) = p(\mathbf{y}_i | \mathbf{t}_i, k_i, \Theta) p(\mathbf{t}_i | \alpha_i) \pi_{ik}. \quad (4)$$

By using an Expectation Maximization (EM)-approach, the model parameters are inferred together with the posterior probabilities of the latent tumor states and normal tissue classification. For a rigorous overview of the method, the reader is referred to [1].

2.2. Split Bregman method

2.2.1. Intensity model

Normal and tumorous tissue intensities are modelled separately. Let $\mathcal{N}(\cdot; \Theta_k^c)$ be a multivariate Gaussian distribution with mean and covariance matrix summarized by Θ , then normal and tumorous tissue are both modelled by a Gaussian mixture model

$$p(\mathbf{y}_i | \Theta) = \sum_k^K \mathcal{N}(\mathbf{y}_i; \Theta_k) p(\Gamma_i = k). \quad (5)$$

The intensity model parameters $\Theta = \{(\mu_k, \Sigma_k) | k \in 1, \dots, K\}$ are iteratively estimated using an EM-approach. For normal tissue, $K = 3$ and $p(\Gamma_i = k) = \pi_{ik}$ are the spatial priors for white matter (WM), grey matter (GM) and cerebro-spinal fluid (CSF). For tumorous tissue, the weights of the Gaussians are updated according to the volume fraction of each of the tumor classes.

2.2.2. Level-set formulation

The image I is partitioned into a (possibly disjoint) tumor region labelled Ω_{in} and a normal region Ω_{out} . The intensities within each region are modelled by the probability distributions described in Sec. 2.2.1. The regions are separated by a boundary $\partial\Omega$ that is implicitly represented by a level-set function. The boundary as well as the intensity model parameters are found by minimizing the energy functional [5]

$$\arg \min_{\Theta_{in}, \Theta_{out}, \partial\Omega} \lambda \int_{\Omega_{in}} -\log p_{in}(I | \Omega_{in}, \Theta_{in}) d\mathbf{x} + \lambda \int_{\Omega_{out}} -\log p_{out}(I | \Omega_{out}, \Theta_{out}) d\mathbf{x} + \text{length}(\partial\Omega). \quad (6)$$

The first two terms penalize the negative log-likelihood of the image I evaluated in respectively the tumor and normal region. The third term penalizes the length of the boundary. Parameter λ determines the relative importance of the data-fitting terms with respect to the regularization term.

2.2.3. Split Bregman method for L_1 -regularized problems

Level-set energy functionals with a length-regularization term as in Eq. 6 are non-convex and a gradient flow on these functionals often converges towards unwanted local optima. Typically, a manual initialization is required that is sufficiently close to the desired solution [6]. Chan et al. [7] reformulated the energy functional as an L_1 -regularized problem, and thereby making it convex. The split Bregman iteration technique was recently proposed for solving this kind of convex problem in a fast and efficient way [4]. As a result, our method will search for tumorous voxels in a global way and independently of a manual initialization. The energy functional equals

$$\arg \min_{0 \leq u \leq 1} \|\nabla u\|_{L_1} + \lambda \langle u, r \rangle \quad (7)$$

with $\langle \cdot, \cdot \rangle$ the summation over the voxel-wise products of the arguments, u is the level-set function and r is the data-fitting term,

$$r = \log p_{out}(I | \Omega_{out}, \Theta_{out}) - \log p_{in}(I | \Omega_{in}, \Theta_{in}). \quad (8)$$

To solve this minimization problem, the split Bregman iteration technique introduces an auxiliary variable $\mathbf{d} = \nabla u$

and the Bregman variable \mathbf{b} and solves a sequence of unconstrained problems

$$(u^{n+1}, \mathbf{d}^{n+1}) = \arg \min_{0 \leq u \leq 1, \mathbf{d}} \|\mathbf{d}\|_{L_1} + \lambda \langle u, r^n \rangle + \frac{\mu}{2} \|\mathbf{d} - \nabla u - \mathbf{b}^n\|^2, \quad (9)$$

$$\mathbf{b}^{n+1} = \mathbf{b}^n + \nabla u^n - \mathbf{d}^n, \quad (10)$$

where u^{n+1} is found by a Gauss-Seidel sweep and \mathbf{d} is found by vectorial shrinkage. The superscript n denotes the iteration index. A more detailed description on the split Bregman iteration technique can be found in [4].

2.2.4. Overall method

An overview of the full method is given in **Algorithm 1**. We remark that for each update of the level-set, a full EM-estimation of the parameters Θ_{in} and Θ_{out} is done.

```

Initialize  $\mathbf{d} = 0, \mathbf{b} = 0, u = 0.5$ 
while  $\|u^{n+1} - u^n\|_{L_2} > \epsilon$  do
    // data-fitting term
     $r^n = \log p_{out}(I|\Omega_{out}^n, \Theta_{out}^n) - \log p_{in}(I|\Omega_{in}^n, \Theta_{in}^n)$ 

    // update level-set from Eq. 9
    Solve  $u^{n+1}$ 
    Solve  $\mathbf{d}^{n+1}$ 
     $\mathbf{b}^{n+1} = \mathbf{b}^n + \nabla u^n - \mathbf{d}^n$ 

    // update regions
     $\Omega_{in}^{n+1} = \{\mathbf{x} : u^{n+1}(\mathbf{x}) > 0.5\}$ 
     $\Omega_{out}^{n+1} = \{\mathbf{x} : u^{n+1}(\mathbf{x}) < 0.5\}$ 

    while EM not converged do
        // update intensity models
         $\Theta_{in}^{n+1}$  from region  $\Omega_{in}^{n+1}$ 
         $\Theta_{out}^{n+1}$  from region  $\Omega_{out}^{n+1}$ 
    end
end

```

Algorithm 1: Split Bregman tumor segmentation method

2.3. Split Bregman method (variant)

As was suggested by Riklin-Raviv et al. [6], the level-set can be replaced by a single level-set for each channel c . Although every level-set can move independently from the others, it is constrained by a tumor probability atlas α that is shared across channels (as is the case in the Bayesian method). The data-fitting term for each level-set now becomes

$$r^c = \log p_{out}(I|\Omega_{out}, \Theta_{out}^c) - \log p_{in}(I|\Omega_{in}, \Theta_{in}^c) + \log(1 - \alpha) - \log \alpha. \quad (11)$$

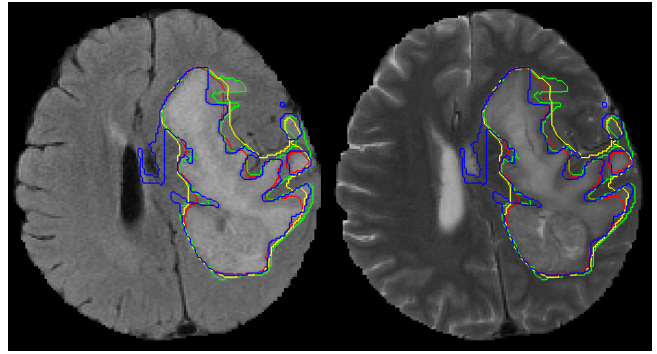


Fig. 1. Segmentation example on FLAIR (left) and T2 (right) high-grade glioma patient nr. 27 with ground truth (green), split Bregman method (red), split Bregman method variant (yellow), and Bayesian method (blue).

3. EXPERIMENTS AND RESULTS

The split Bregman, split Bregman variant and Bayesian method are validated on the training data set of the MICCAI BraTS 2012-2013 Challenge [2]. This training data set comprises 30 glioma patients. For each patient the following MRI channels were acquired: T1-weighted MRI, T1-weighted MRI with contrast enhancement (T1c), T2-weighted MRI and T2-weighted MRI with Fluid-Attenuated Inversion Recovery (FLAIR). All images were skull-stripped and rigidly registered to the T1c image for each patient. Expert annotations of the whole tumor volume were also provided.

Pre-processing of the images includes bias field correction of all MR modalities and an erosion of the provided brain mask by a $1 \times 1 \times 1$ mm ball to exclude spurious non-brain voxels. The prior probabilities of WM, GM and CSF from the publicly available Colin 27 Average Brain atlas [8] are non-rigidly registered to the patient image and are smoothed by a $1 \times 1 \times 1$ mm Gaussian kernel. Spurious non-pathological outliers (image artefacts) are removed in a post-processing step: connected components that are hypo-intense in the T2 or FLAIR image compared to the average gray matter intensity are removed, after which only the largest connected component is retained. Results are reported with and without this post-processing step. Initialization of the Bayesian method as it was originally proposed by Menze et al. is found to work counter-productive and is replaced with the initial assumption that it is equally probable that a voxel is tumorous or normal. The split Bregman method parameters from Eq. 9 are set to $\lambda = \mu = 1e1$. Although a full parameter tuning report is out of the scope of this work, the value of the parameters λ and μ are of little influence to the segmentation result. For the Bayesian method, the Markov Random Field-strength parameter β is set to $\beta = 1$ as was suggested by Menze et al.

The computation time for a single patient volume is about 15 minutes on a 2x2.66Ghz Quad-Core CPU, out of which 10

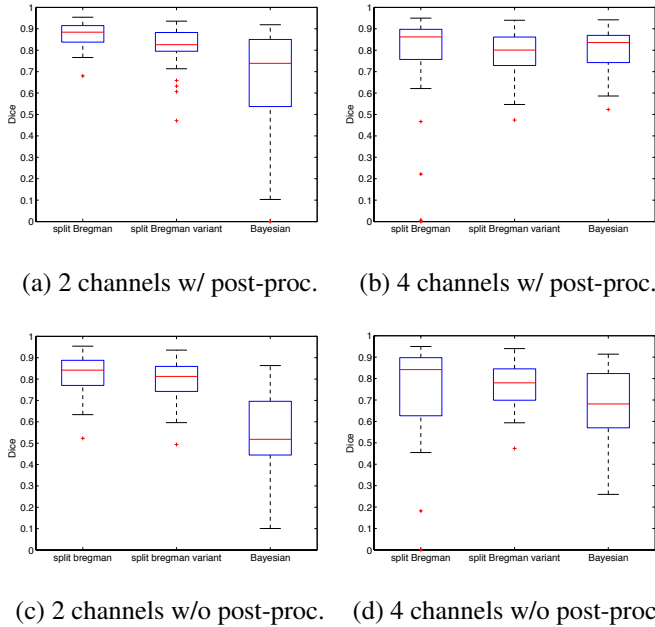


Fig. 2. Dice scores for segmentation results with post-processing (a and b) and without post-processing (c and d). Segmentations are based only on T2 and FLAIR (a and c), or all four channels (b and d).

minutes are spent on the non-rigid registration of the priors to the patient volume. A segmentation example for the split Bregman, the split Bregman variant and Bayesian method is visualized in Fig. 1. The distributions of the Dice scores are reported in Fig. 2. As the whole tumor volume is best visible in the T2 and FLAIR images, we segment the tumor based only on the T2 and FLAIR images (Fig. 2 a and c) and based on all four channels (Fig. 2 b and d). By means of the paired Wilcoxon signed rank test with 5% significance level, we state the following: for the split Bregman and split Bregman variant method, it is better to use two channels instead of four channels based on the post-processed results. This is also true for the split Bregman variant results without post-processing. Although, if we choose to use all four channels, the results are insufficient to state that split Bregman performs better than split Bregman variant or vice versa. For the Bayesian method, results based on all four channels are better than those based on only two channels. Finally, we can state that the split Bregman method performs significantly better than the Bayesian method. Segmentation by the split Bregman method on the T2 and FLAIR images has a median and average Dice score of 0.88 and 0.87 ± 0.06 respectively. Segmentation by the Bayesian method on all channels has a median and average score of 0.83 and 0.80 ± 0.10 . In comparison, the inter-rater variation of the MICCAI BraTS 2012-2013 Challenge annotations (training and testing data set combined) has a median and average Dice score of 0.87 and 0.85 ± 0.08 [2].

4. DISCUSSION AND CONCLUSION

In this work we have presented an untrained and unsupervised MRI brain tumor segmentation method, which makes the method well suited for clinical or research settings for which only a limited amount of patient images needs to be segmented, or not sufficient annotated training data are available. The problem is formulated as an L_1 -regularized optimization problem and is solved by a split Bregman iteration technique, which guides the search for outlier voxels towards a global optimum. By using spatial priors of WM, GM and CSF, this global optimum coincides with the clinically meaningful notion of normal and tumorous regions. On the BraTS 2012-2013 training data, the presented method performs better than the unsupervised Bayesian method by Menze et al.

5. REFERENCES

- [1] B.H. Menze, K. Van Leemput, D. Lashkari, M.A. Weber, N. Ayache, and P. Golland, "A generative model for brain tumor segmentation in multi-modal images.," *MICCAI*, vol. 13, no. Pt 2, pp. 151–159, 2010.
- [2] B. Menze, M. Reyes, and K. Van Leemput, "The multimodal brain tumor image segmentation benchmark.," *IEEE TMI*, vol. 34, no. 10, pp. 1993–2024, 2014.
- [3] K. Van Leemput, F. Maes, D. Vandermeulen, and P. Suetens, "Automated Model-Based Tissue Classification of MR Images of the Brain.," *IEEE TMI*, vol. 18, pp. 897–908, 1999.
- [4] T. Goldstein, X. Bresson, and S. Osher, "Geometric applications of the split bregman method: Segmentation and surface reconstruction.," *Journal of Scientific Computing*, vol. 45, no. 1-3, pp. 272–293, 2010.
- [5] M. Rousson and R. Deriche, "A variational framework for active and adaptative segmentation of vector valued images.," in *Workshop on Motion and Video Computing*. 2002, MOTION '02, pp. 56–62, IEEE Computer Society.
- [6] T. Riklin-Raviv, K. Van Leemput, B.H. Menze, W.M. Wells, and P. Golland, "Segmentation of image ensembles via latent atlases.," *Medical Image Analysis*, vol. 14, no. 5, pp. 654–665, 2010.
- [7] T.F. Chan, S. Esedoglu, and M. Nikolova, "Algorithms for finding global minimizers of image segmentation and denoising models.," *SIAM Journal on Applied Mathematics*, vol. 66, no. 5, pp. 1632–1648, 2006.
- [8] C.J. Holmes, R. Hoge, L. Collins, R. Woods, A.W. Toga, and A.C. Evans, "Enhancement of MR images using registration for signal averaging.," *J Comput Assist Tomogr*, vol. 22, no. 2, pp. 324–333, Mar-Apr 1998.